

Enhanced confinement regimes with strong electron heating in the presence of flat or inverted safety factor profiles

F Alladio†, B Angelini†, M L Apicella†, G Apruzzese†, E Barbato†, M R Belforte†, L Bertalot†, A Bertocchi†, M Borra†, G Bracco†, A Bruschi‡, G Buceti†, P Buratti†, A Cardinali†, C Castaldo†, C Centioli†, R Cesario†, P Chuilon†, C Cianfarani†, S Ciattaglia†, S Cirant‡, V Cocilovo†, F Crisanti†, R De Angelis†, F De Marco†, B Esposito†, D Frigione†, L Gabellieri†, G Gatti†, E Giovannozzi†, C Gourlan†, F Gravanti†, G Granucci‡, B C Gregory§, M Grolli†, F Iannone†, H Kroegler†, M Leigheb†, G Maddaluno†, G Maffia†, M Marinucci†, G Mazzitelli†, P Micozzi†, F Mirizzi†, F P Orsitto†, D Pacella†, L Panaccione†, M Panella†, V Pericoli-Ridolfini†, L Pieroni†, S Podda†, G B Righetti†, F Romanelli†, F Santini†, M Sassi†, S E Segre||, E Sternini†, A Simonetto‡, C Sozzi‡, N Tartoni†, B Tilia†, A A Tuccillo†, O Tudisco†, V Vitale†, G Vlad†, V Zanza†, M Zerbini† and F Zonca†

† Associazione EURATOM-ENEA sulla Fusione, CRE Frascati, 00044, Frascati, Roma, Italy

‡ Associazione EURATOM-ENEA-CNR sulla Fusione Milano, Italy

§ Institut National de la Recherche Scientifique (INRS), Montreal, Canada

|| II Università di Roma 'Tor Vergata', Rome, Italy

Received 3 July 1998

Abstract. The role of magnetic shear in affecting electron transport is discussed on the basis of the Frascati tokamak upgrade (FTU) data with central electron cyclotron resonance heating (ECRH) on the current ramp phase and with pellet injection. The results point out that strongly negative magnetic shear is not a necessary condition in order to have good electron transport and that magnetohydrodynamic (MHD) activity plays a crucial role in affecting the electron transport in the region with low/negative magnetic shear. The theoretical arguments for the dependence of transport on magnetic shear are reviewed and compared with the experimental evidence.

1. Introduction

The possibility of achieving enhanced confinement regimes in the presence of flat or inverted safety factor profiles has been demonstrated by several tokamaks in the last few years [1–10]. These regimes are potentially interesting in view of the application to the advanced mode of tokamak operation characterized by a large fraction of the plasma current produced by the bootstrap mechanism which tends to yield non-monotonic safety factor profiles.

In most of the experiments carried out so far, the confinement improvement is mainly associated with the ion channel whereas the electron confinement does not seem to be strongly affected, except in the case of large negative magnetic shear discharges on JT-60U [3] and optimized shear discharges on JET [4]. Furthermore, most of the results refer to a situation characterized by dominant ion heating, whereas only a minor number of experiments have

observed such a result with dominant electron heating, which is the typical situation of an alpha particle heated reactor plasma. To be specific, a reduction of the electron thermal conductivity has been observed in Tore Supra with lower hybrid (LH) current drive [8] and on RTP with electron cyclotron resonant heating (ECRH) [10]. However, in both cases the low/reversed magnetic shear equilibrium is obtained in the presence of off-axis heating, making it difficult to determine the transport behaviour in the presence of large gradients in the temperature profile which can provide enough free energy to drive the electron turbulence.

In the present paper, the following issues will be addressed: (a) Is strong negative shear necessary to obtain enhanced confinement? (b) Is the improvement characterized by a barrier or by a global decrease? (c) What is the role of magnetohydrodynamic (MHD) activity in affecting the electron transport?

In order to investigate these points, discharges with low/reversed magnetic shear obtained either by ECRH on the current ramp [9] or pellet injection [11] have been performed on the Frascati tokamak upgrade (FTU) (major radius $R_0 = 0.935$ m, minor radius $a = 0.3$ m, molybdenum toroidal limiter, stainless steel liner) [12]. The use of central ECRH, in the presence of flat/non-monotonic q profiles, allows us to produce large electron temperature gradients which can, in principle, destabilize electron turbulence. Pellet injection discharges exhibit extended phases in which no macroscopic MHD activity is present and allow for good power balance analysis. It should be noted that the first example of confinement enhancement with flat/non-monotonic q profiles has indeed been observed on JET with pellet injection [13]. A comprehensive analysis of the MHD activity in these FTU discharges is presented in [14].

The plan of the paper is as follows. In section 2 the FTU results with ECRH are described and discussed. The role of MHD activity is investigated in section 3 both for ECRH and pellet discharges. In section 4 the theoretical arguments are reviewed which support an explicit dependence on magnetic shear of the electron transport. Concluding remarks are given in section 5.

2. Electron cyclotron heating on the current ramp

Experiments were carried out on FTU by injecting up to 360 kW of ECRH power at 140 GHz (corresponding to the fundamental electron cyclotron frequency at $B = 5$ T) during the current ramp-up phase of 0.7 MA discharges. Profiles with reversed magnetic shear were obtained by ramping the plasma current at a fast rate ($5\text{--}7$ MA s⁻¹) in the presence of high electron temperature values (in excess of 8 keV) that slow down the current diffusion.

The time evolution of a typical deuterium discharge is shown in figure 1. The toroidal magnetic field at the centre of the vacuum chamber was set at $B_0 = 5.4$ T in order to have the resonance close to the magnetic axis ($R_{\text{ax}} = 0.97$ m). Temperature and density at the beginning of the ECRH pulse ($t = 55$ ms) were $T_e(R_{\text{ax}}) = 1$ keV and $n_e(R_{\text{ax}}) = 2.5 \times 10^{19}$ m⁻³. The central temperature reached a steady state in 25 ms.

Resistive diffusion calculations show that a non-monotonic q profile was produced during most of the ECRH pulse. A fast rearrangement in the temperature profile involving an annular region is observed at $t = 106$ ms, with $m = 2$ post cursor oscillations, which can be attributed to the destabilization of a double tearing mode in the presence of a pair of $q = 2$ MHD resonances [14]. This observation confirms that a non-monotonic q profile is indeed achieved. The T_e profile evolution for the same discharge is shown in figure 2.

The power balance in the central region of the discharge shown in figure 2 is dominated by ECRH since the achieved flux surface averaged ECRH power densities are larger by an order of magnitude than the ohmic values, due to good collimation of the launched beam, the low plasma refraction and the very high first pass absorption [15]; this allows us to perform an

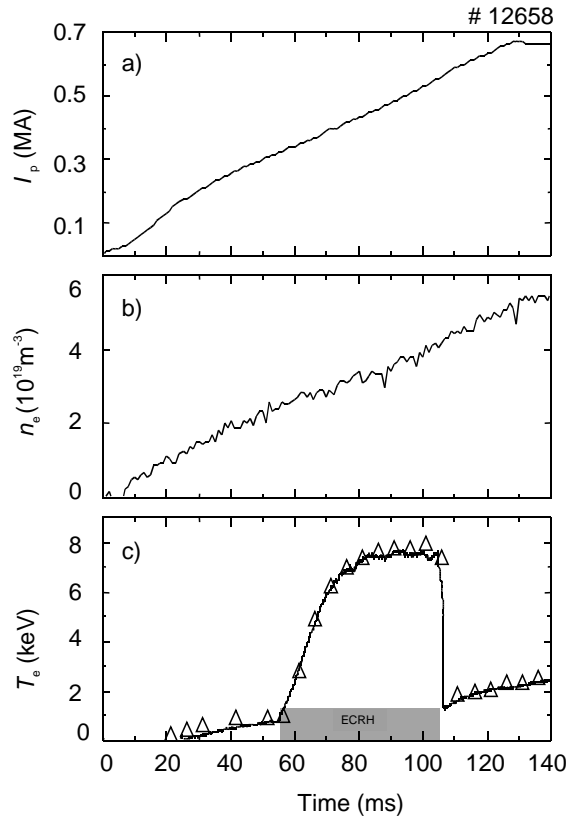


Figure 1. Time evolution of (a) plasma current; (b) line-averaged electron density; (c) fast electron temperature measurement at $R = 1.01$ m (full curve) and peak temperature (triangles).

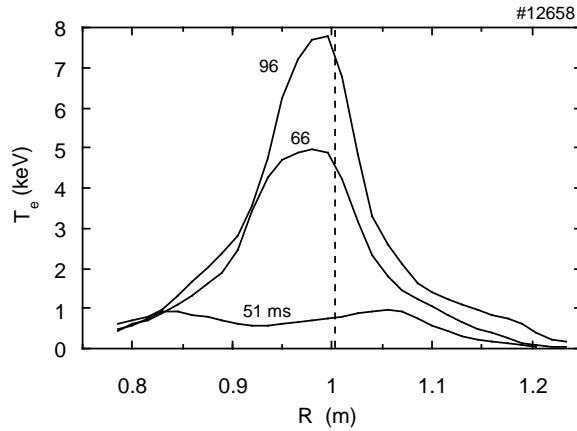


Figure 2. Electron temperature profile evolution for the pulse shown in figure 1. ECRH is applied at $t = 55$ ms; the resonance location is marked by a broken vertical line.

accurate analysis of the electron heat transport in a plasma with reversed magnetic shear and large values of the heat flux.

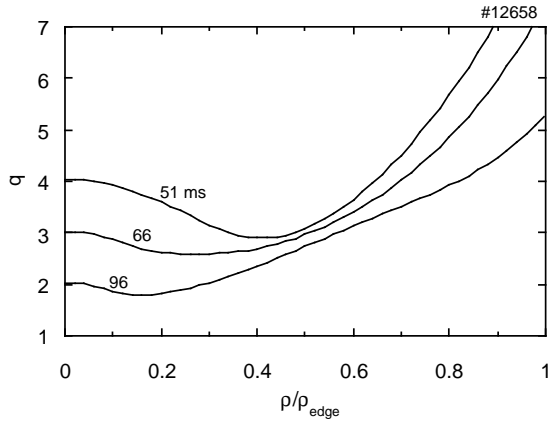


Figure 3. Time evolution of the q profile calculated for pulse 12658 assuming $Z_{\text{eff}} = 6.7$, Spitzer resistivity and relaxed current profile at $t = 51$ ms.

The electron thermal diffusivity χ_e is obtained (by neglecting convective losses) from the condition

$$\langle q_e \nabla \rho \rangle = -\chi_e n_e \langle |\nabla \rho|^2 \rangle \frac{\partial T_e}{\partial \rho}.$$

The left-hand side is the radial component of the electron heat flux averaged on the magnetic surface and can be evaluated from the electron power balance equation:

$$\langle q_e \nabla \rho \rangle = (P_{\text{EC}} + P_{\text{OH}} - P_{\text{ei}} - P_{\text{RAD}} - \partial W / \partial t) / V'$$

which accounts for power sources and sinks inside the magnetic surface: P_{EC} is the ECRH power, P_{OH} is the ohmic power, P_{ei} is the electron–ion equipartition term, P_{RAD} is the radiated power, W is the electron thermal energy and $V' = \partial V / \partial \rho$. The effective flux surface radius $\rho = \sqrt{\Phi_T / \pi B_0}$ is defined in terms of the toroidal flux Φ_T . The experimental equilibrium is determined by a magnetic reconstruction code [16].

The q -profile evolution for pulse 12658 (see figure 2) is shown in figure 3. The profiles are obtained from the solution of the magnetic field diffusion equation, starting with a relaxed current density profile at $t = 51$ ms, i.e. neglecting the skin effect in the low-temperature phase which precedes the ECRH injection. The calculation is benchmarked by the occurrence of a $m = 2$ double tearing relaxation at $t = 106$ ms.

The electron thermal diffusivity profile is shown in figure 4. The uncertainties arising from the ohmic power evaluation, represented by the shaded area in the figure, are reasonably low for $\rho / \rho_{\text{edge}} < 0.4$. It is remarkable that the diffusivity values are below $0.4 \text{ m}^2 \text{ s}^{-1}$ in the region inside one third of the plasma radius with a minimum at $\chi_e \approx 0.2 \text{ m}^2 \text{ s}^{-1}$; such values are close to the lowest ones found in ohmic discharges, but have now been obtained in the presence of much larger fluxes and electron temperature gradients, as shown in figure 5, where the electron heat flux against $-n_e \partial T_e / \partial \rho$ plots are overlaid for the pulse 12658 at $t = 96$ ms (at this time $I_p = 0.5 \text{ MA}$ and $\bar{n}_e = 4 \times 10^{19} \text{ m}^{-3}$), and for two typical ohmic, steady-state discharges with similar current and density.

3. Effect of MHD activity on the electron transport

The electron energy confinement in plasma regions with low or reversed magnetic shear is limited by MHD activity. This is evident in ECRH discharges, in which the progressive

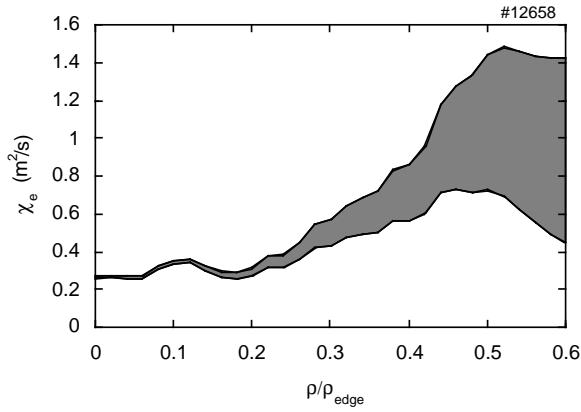


Figure 4. Radial profile of the electron heat diffusivity for pulse 12658 at $t = 96$ ms. The shaded area represents the uncertainties arising from the ohmic power calculation.

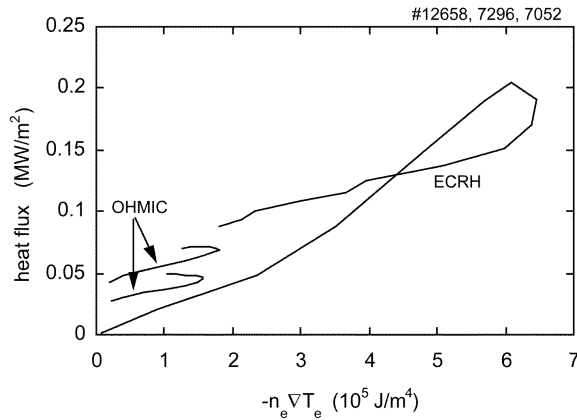


Figure 5. Flux surface averaged normal electron heat flux against $-n_e \partial T_e / \partial \rho$ for pulse 12658 at $t = 96$ ms and for the flat-top of two ohmic pulses with similar current and density (7052, $t = 880$ ms; 7296, $t = 980$ ms). SI units are used so that, apart from a geometric factor close to 1, χ_e is just the ratio between the plotted quantities. Data are shown for $\rho \leq 0.3\rho_{\text{edge}}$.

decrease of the minimum q value (q_{min}) is accompanied by macroscopic (5–10% amplitude) temperature fluctuations (figure 6). For $q_{\text{min}} \approx 1$, the temperature evolution transiently reverts from fluctuating to monotonically increasing, and the thermal energy in the plasma core increases at a rate of 260 kW, which is close to 70% of the net power input in the same plasma volume; as a consequence, the electron thermal diffusivity given by the interpretative transport analysis is strongly reduced throughout the plasma core. Figure 7 shows that such a reduction is due not only to the reduced heat flux, but also to an increase in the temperature gradient. The shear calculated from the magnetic field diffusion equation ranges from $s = 0$ to $s = 0.3$ in the low transport region. This demonstrates that a strongly negative shear is not a necessary condition for low electron transport.

The observation of confinement improvement associated with a pause in macroscopic fluctuations points to the existence of energy transport due to non-diffusive, intermittent phenomena, that play a role similar to sawteeth, although their period is erratic, and their amplitude is sufficient to clamp the peak temperature, but not to flatten the profile in the central region.

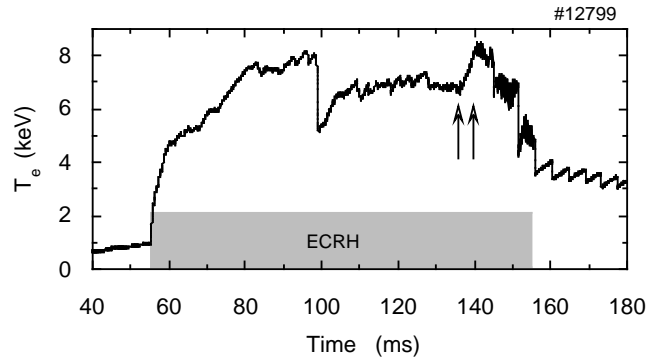


Figure 6. Time traces of $T_e(0)$ for FTU pulse 12799 with $P_{\text{ECRH}} = 360$ kW. The arrows mark the times for the profiles shown in figure 8.

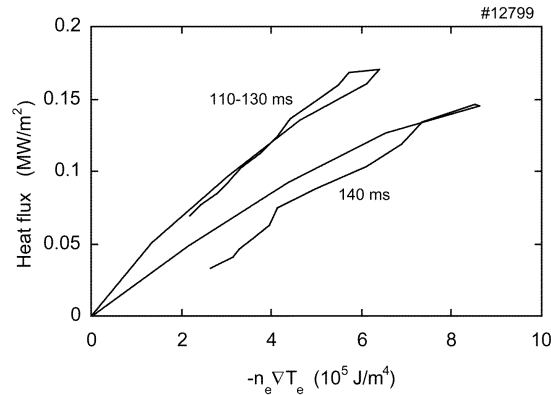


Figure 7. Flux surface averaged normal electron heat flux against $-n_e \partial T_e / \partial \rho$ for pulse 12799 before and during the T_e rise at $q_{\text{min}} = 1$. SI units are used so that, apart from a geometric factor close to 1, χ_e is just the ratio between the plotted quantities. Data are shown for $\rho \leq 0.3\rho_{\text{edge}}$.

The temperature rise in the discharge shown in figure 6 lasts for about 10 ms, just enough to estimate its effect on the power balance, the time resolution of the temperature profile measurement being 5 ms (figure 8).

A similar phenomenon is observed a short time before the onset of sawteeth in all FTU discharges with central ECRH. The temperature rise is terminated by the onset of $m = 1$ oscillations that precur the first sawtooth crash. A similar phenomenon has been observed on the DIII-D tokamak during fast wave injection experiments [17].

A temperature rise is also observed for $q_{\text{min}} \approx 2$, provided that the minimum q radius is close to the magnetic axis (this is not the case of figure 6, where the negative shear region is relatively broad when $q_{\text{min}} \approx 2$, and a large scale double tearing crash is observed instead of the temperature rise). The duration of this phenomenon is not sufficient to detect its effect on the power balance, but the correlation between the temperature rise and the pause in fluctuations, followed by a rapid temperature drop caused by the growth of an $m = 2$ magnetic island is clear [14b].

Improvements of the electron confinement associated to integer or half-integer q values had been observed in other experiments [18] and been attributed to the existence of transport barriers. On the other hand, increased transport due to the formation of magnetic islands has

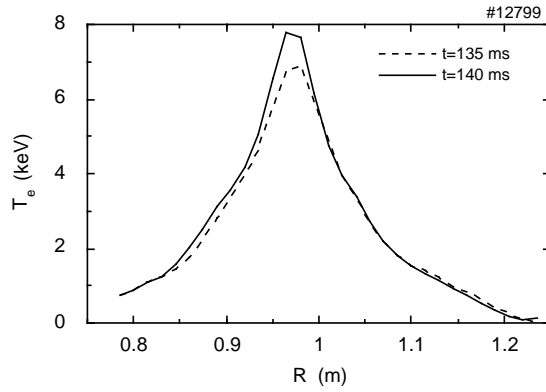


Figure 8. Temperature profiles before and during the T_e rise at $q_{\min} = 1$ phase for FTU pulse 12799.

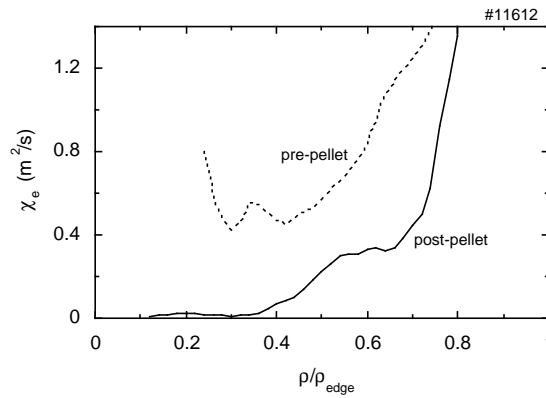


Figure 9. Electron thermal diffusivity before pellet injection (broken curve) and during the MHD-quiescent phase (full curve) for FTU pulse 11612. The pre-pellet data are not plotted in the region affected by sawteeth.

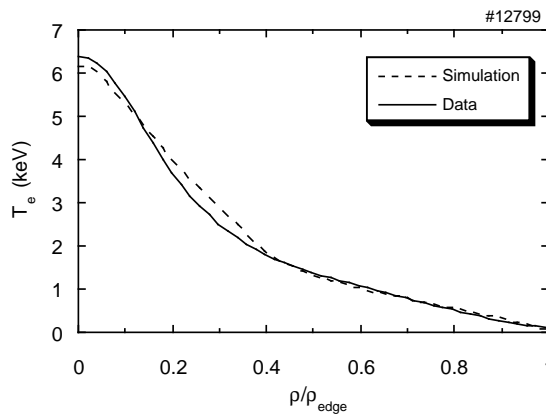


Figure 10. Comparison between the temperature profile measured at $t = 130$ ms in pulse 12799 and the one simulated by the mixed Bohm-gyro-Bohm transport model.

also been observed in several experiments with monotonic q profiles. The picture emerging from FTU results bridges the gap between those apparently contradictory observations: for inverted or flat q profiles, the purely diffusive electron heat flux is very low, but the temperature peaking is clamped by macroscopic fluctuations. For the major ones occurring at $q_{\min} \approx 1$ and $q_{\min} \approx 2$, the behaviour of the temperature time-traces allows to ascribe the temperature drops to the destabilization of tearing modes. We conjecture that all the observed macroscopic fluctuations are due to the excitation of tearing modes as q_{\min} crosses low-order rational values, and that the absence of such values in gaps around integer q_{\min} values is the reason for the confinement improvement. Tearing modes with $m > 2$ can be destabilized owing to the presence of pairs of $q = m/n$ resonances if the shear is negative [14]. In addition, the large pressure gradient can bring the system close to the ideal stability threshold: the local poloidal beta $\beta_p(r) = 2\mu_0(\langle p \rangle - p(r))/B_p(r)^2$ can reach values $\beta_p > 3$ in the low-negative shear region. On the other hand, near-integer q values do not play any positive role where the q profile is monotonic and the pressure gradient is lower due to strongly anomalous diffusive transport, so that only the adverse effect of islands at exactly integer q values is left.

The confinement improvement in ECRH discharges is transient, since the q profile evolution is driven on the resistive diffusion time scale by the current ramp-up. The injection of deuterium pellets penetrating inside the sawtooth inversion radius suppresses the sawtooth activity and leaves the plasma MHD-quiescent for at least one confinement time. This allows us to study the diffusive heat transport in a wide plasma region of nearly zero magnetic shear. Transport analysis shows that the electron heat transport is almost suppressed in this region [11] as shown in figure 9. The MHD-quiescent period is terminated by the growth of an $m = 1$, $n = 1$ kink distortion of the plasma core. According to resistive diffusion calculations, the central q rises slightly above the pre-pellet value during the quiescent period, and decreases again just before the onset of the $m = 1$ mode. This result suggests that the suppression of electron heat transport in the post-pellet phase is due to the same effective transport barrier that has been found in ECRH discharges for $q_{\min} \approx 1$.

4. Theoretical models for confinement improvement

The aim of the present section is to review the theoretical arguments which support an explicit dependence of the turbulent electron transport on magnetic shear. The $(E \times B)$ stabilization mechanism [19], which qualitatively explains most of the features of the transitions, has been reviewed in [20] and will not be further discussed here.

4.1. Change in the toroidal precession velocity

In the presence of negative magnetic shear, the toroidal precession frequency of trapped particles changes sign and the wave-particle resonance condition is lost for modes propagating in the electron diamagnetic direction. As shown first by Kadomtsev and Pogutse [21], as magnetic shear is decreased, the region in velocity space corresponding to a negative precession velocity increases in size. As a consequence, modes propagating in the electron diamagnetic direction tend to loose the wave-particle resonance condition and the collisionless trapped electron mode tends to be suppressed.

This result is particularly interesting in view of the explanation of the confinement enhancement obtained with pellet injection. It was shown in [22] that peaking the density profile is effective in order to stabilize the ion temperature gradient driven mode only as long as the effect of trapped electrons is suppressed. Such a result may be obtained if the electron collisionality is sufficiently large that the trapped-electron population is reduced, but certainly

this is not the case, for example, for the pellet enhanced performance mode on JET [13] which achieved conditions in which the collisionless trapped electron mode should be excited. Such a discrepancy can be reconciled with the experimental results if the safety factor profile is hollow. In particular, in the latter case the change in the trapped particle precession frequency can reduce the region corresponding to the residual trapped electron instability shown in figure 3 of [22].

4.2. Changes in the radial correlation length

The radial correlation length of electrostatic turbulence is also strongly affected by magnetic shear. In a 2D tokamak equilibrium a global eigenmode, characterized by a toroidal mode number n , is formed by the superposition of poloidal harmonics with different poloidal mode number m , each harmonic being centred around the magnetic surface at which $q = m/n$. For $s = O(1)$ the distance between neighbouring mode rational surfaces is comparable with the radial width of each poloidal harmonic. As a consequence, the degree of overlap between neighbouring poloidal harmonics is large and the resulting global eigenfunction is characterized by a radial correlation length of the order $L_r \approx (a\rho_i)^{1/2}$, with a being the minor radius and ρ_i the ion Larmor radius [23]. As magnetic shear is decreased, the distance between neighbouring mode rational surfaces increases faster than the width of each harmonic. As a consequence the degree of overlap becomes small and each poloidal harmonic tends to behave independently of the neighbouring harmonics. In these conditions the radial correlation length decreases exponentially as shear is decreased $L_r \approx (a\rho_i)^{1/2} \exp(-1/|s|)$, approaching a value corresponding to the width of a single harmonic, which scales as the ion Larmor radius. Upon assuming that the thermal diffusivity is given by quasilinear theory

$$\chi_e = \frac{L_r^2}{\tau_c}$$

with τ_c being the turbulence autocorrelation time, this expression takes the form of a Bohm and a gyro-Bohm diffusion coefficient in the high and low magnetic shear limit, respectively. On the basis of this theoretical argument, a mixed Bohm–gyro-Bohm model has been proposed which accounts for the shear dependence of transport [24]

$$\chi_e = D_B(a/L_T)(\alpha_B q^2 f(s) + \alpha_{gB} \rho^*)$$

with $D_B = T_e/eB$ is the Bohm coefficient, $L_T = -(d \ln T_e/dr)^{-1}$, $\rho^* = \rho_s/a$, ρ_s is the ion Larmor radius evaluated with the electron temperature, α_B and α_{gB} are numerical coefficients and $f(s) = s^2/(1+|s|^3)$. The model has been validated against JET data and the ITER database. A comparison with FTU data is shown in figure 10 showing reasonably good agreement.

The two mechanisms discussed have different implications. The former requires strongly negative magnetic shear values for the transport barrier formation, whereas the latter requires a low magnetic shear value for transport improvement, in agreement with the FTU results.

It is important to note that the mechanisms discussed are not alternative to the explanation of the onset of transport barriers in terms of the formation of radial electric fields which induce a sheared ($E \times B$) rotation to quench the plasma turbulence. In addition, negative magnetic shear can also enhance the ($E \times B$) shearing rate [25]. Finally, the high- q values in the plasma core typical of these regimes may produce an enhanced Shafranov shift which plays a stabilizing role on the ion temperature gradient driven modes [26].

5. Discussion and conclusions

The analysis of ECRH and pellet discharges on FTU shows that, in order to improve the electron transport, the presence of a strongly negative magnetic shear (as inferred from the

JT60-U results) is not a necessary condition. As discussed in [27], the correlation with the presence of a strongly negative magnetic shear region could be due to the very slow current diffusion following the onset of the electron transport barrier. The interplay between current diffusion and electron transport barrier formation makes difficult a precise assessment of the specific role of magnetic shear.

A decrease in the electron thermal conductivity is observed on FTU over the entire region of small/negative magnetic shear. It is remarkable that such a low value is observed in the presence of a large temperature gradient which can provide a substantial free energy source to drive electron turbulence. Therefore, the present result goes beyond the conventional improvement obtained simply by sawtooth stabilization and limited to the region inside the $q = 1$ surface.

The role of MHD activity is crucial in affecting the electron transport. During the phase in which MHD activity is totally suppressed the electron transport drops to very low values in the presence of flat or inverted q profiles. Such a behaviour is particularly impressive in pellet discharges which exhibit an extended phase with negligible electron transport.

References

- [1] Levinton F M et al 1995 *Phys. Rev. Lett.* **75** 4417
- [2] Strait E J et al 1995 *Phys. Rev. Lett.* **75** 4421
- [3] Fujita T, Ide S, Shirai H, Kikuchi M, Naito O, Koide Y, Takeji S, Kubo H and Ishida S 1997 *Phys. Rev. Lett.* **78** 237
- [4] Jones T T C and the JET Team 1997 *Phys. Plasmas* **4** 1725
- [5] Koide Y and the JT-60 Team 1997 *Phys. Plasmas* **4** 1623
- [6] Greenfield C M et al 1997 *Phys. Plasmas* **4** 1596
- [7] Burrell K H 1997 *Phys. Plasmas* **4** 1499
- [8] Litaudon X et al 1996 *Plasma Phys. Control. Fusion* **38** 1603
- [9] Barbato E et al 1997 *Proc. 24th Eur. Conf. on Controlled Fusion and Plasma Physics (Berchtesgaden, Germany)* vol 21A (Geneva: European Physical Society) p 1161
- [10] de Baar M R, Hogewij G M D, Lopes Cardozo N J, Oomens A A M and Schüller F C 1997 *Phys. Rev. Lett.* **78** 4573
- [11] Bracco G et al 1994 *Proc. 21th Eur. Conf. on Controlled Fusion and Plasma Physics (Montpellier, France)* vol 18B (Geneva: European Physical Society) part I, p 142
Frigione D et al 1997 *Proc. 24th Eur. Conf. on Controlled Fusion and Plasma Physics (Berchtesgaden, Germany)* vol 21A (Geneva: European Physical Society) p 1177
- [12] Andreani R et al 1990 *Fusion Technology (Proc. 16th Symp. London 1990)* vol 1 (Amsterdam: North-Holland) p 218
- [13] Balet B et al 1990 *Nucl. Fusion* **30** 2029
- [14] Buratti P et al 1997 *Plasma Phys. Control. Fusion* **39** B383
Buratti P et al these proceedings
- [15] Cirant S et al 1997 *Proc. 10th Joint Workshop on ECE and ECRH* ed T Donnè and T Verhoeven, p 369
- [16] Alladio F and Micozzi P 1997 *Nucl. Fusion* **35** 805
- [17] Forest C B et al 1996 *Phys. Rev. Lett.* **77** 3141
- [18] Lopes Cardozo N J et al 1997 *Plasma Phys. Control. Fusion* **39** B303
- [19] Biglari H, Diamond P H and Terry P W 1990 *Phys. Fluids B* **2** 1
- [20] Synakowski E J 1998 *Plasma Phys. Control. Fusion* **40** 581
- [21] Kadomtsev B B and Pogutse O P 1966 *Zh. Eksp. Teor. Fiz.* **51** 1734 (Engl. Transl. *Sov. Phys.–JETP* **24** 1172)
- [22] Romanelli F and Briguglio S 1990 *Phys. Fluids B* **2** 754
- [23] Romanelli F and Zonca F 1993 *Phys. Fluids B* **5** 4081
Connor J W, Taylor J B and Wilson H R 1993 *Phys. Rev. Lett.* **70** 1803
- [24] Vlad G, Marinucci M, Romanelli F, Cherubini A, Erba M, Parail V V and Taroni A 1998 *Nucl. Fusion* **38** 557
- [25] Hahm T S and Burrell K H 1995 *Phys. Plasmas* **2** 1648
- [26] Beer M et al 1997 *Phys. Plasmas* **4** 1792
- [27] Koide Y, Burrell K H, Rice B W and Fujita T 1998 *Plasma Phys. Control. Fusion* **40** 97